American Mineralogist, Volume 83, pages 739–745, 1998

Gibbs energies of formation for hydrocerussite [$Pb(OH)_2 \cdot (PbCO_3)_2$(s)] and hydrozincite {$[Zn(OH)_2]_3 \cdot (ZnCO_3)_2$(s)} at 298 K and 1 bar from electrochemical cell measurements

M.A. Mercy,[1,*] Peter A. Rock,[2] William H. Casey,[3] and Mehdi M. Mokarram[2,3]

[1]Department of Geology, University of California, Davis, California 95616, U.S.A.
[2]Department of Chemistry, University of California, Davis, California 95616, U.S.A.
[3]Department of Land, Air, and Water Resources and Department of Geology, University of California, Davis, California 95616, U.S.A.

Abstract

New values are reported for the Gibbs energies of formation from the elements for hydrocerussite $Pb(OH)_2 \cdot (PbCO_3)_2$ and hydrozincite $[Zn(OH)_2]_3 \cdot (ZnCO_3)_2$. These ΔG_f^0 values were obtained from electrochemical cells without liquid junction. We determined ΔG_f^0 [$Pb(OH)_2 \cdot (PbCO_3)_2$(s)] = -1699.8 ± 1.6 kJ/mol for hydrocerussite and ΔG_f^0 {$[Zn(OH)_2]_3 \cdot (ZnCO_3)_2$} = -3163.3 ± 4 kJ/mol for hydrozincite. These results allow future electrochemical cell experiments to be performed to determine the ΔG_f^0 values of other hydroxycarbonate minerals using either the Pb amalgam-hydrocerussite or the Zn amalgam-hydrozincite as reference electrodes. These reference electrodes provide a strategy for establishing Gibbs energies for phases with two different anions, which are geochemically interesting but difficult to study experimentally.

Introduction

Garrels (1957) noted that the paragenesis of some hydroxycarbonate minerals, such as hydrocerussite [$Pb(OH)_2 \cdot (PbCO_3)_2$(s)], was inconsistent with the contemporary thermodynamic data. Hydrocerussite is rare in soils relative to the mineral cerussite [$PbCO_3$(s)], and Garrels adjusted the experimental Gibbs energy of hydrocerussite accordingly. This adjustment remained in the literature for many years until the original results of Randall and Spencer (1928) were augmented by other careful solubility experiments (see Bilinski and Schindler 1982; Taylor and Lopata 1984). Solubility experiments on these solids, however, are enormously difficult because the results are sensitive to the speciation model chosen to interpret the data (see discussion by Bilinski and Schindler 1982). In this paper, we employ an electrochemical cell method to determine the Gibbs energies of formation of hydroxycarbonate minerals simply and directly. The cell method is applied to the environmentally significant mineral hydrocerussite and verified using hydrozincite {$[Zn(OH)_2]_3 \cdot (ZnCO_3)_2$(s)}, but the method can be extended to other hydroxycarbonates, allowing relatively simple Gibbs energy of formation determinations to be made for many of these complex double-anion minerals.

Although hydrocerussite is rare in soils relative to cerussite, hydrocerussite is found to be a weathering product of native Pb (Jørgensen and Willems 1987), which is a potentially enormous environmental hazard. The estimated domestic use of Pb in 1992 was 1 220 000 metric tons (Smith et al. 1995) with over 80% of this Pb used for lead-acid batteries. However, only about 760 000 metric tons of Pb was recovered from such batteries in 1992. The unaccounted Pb was presumably lost to the environment. The dispersion of metallic Pb is going to increase if current zero-emission vehicle policies are enacted in California, Michigan, and Massachusetts. This policy requires that an appreciable fraction (1–2%) of the new vehicles sold in a state must have no detectable emission of air pollutants from the tailpipe (Sperling 1995; Brady et al. 1998). A leading technology proposed to satisfy this policy requires electric cars with lead-acid storage batteries. In addition, hydrocerussite is a surprisingly common precipitate in experimental Pb-Na_2SO_4-$NaHCO_3$ solutions (Marani et al. 1995). In this paper, we return to Garrels' conjecture and use the new thermodynamic data to provide a geochemical explanation for the relative distribution of hydrocerussite and cerussite in soils.

Experimental methods

Solid samples

The hydrocerussite used was a synthetic powder purchased from Mallinckrodt (Lot KMME no. 5709). The hydrozincite used was identified as ''zinc carbonate basic'' by Fluka Chemika (no. 96466, Analysis no. 323007). In one cell (cell D), a sample of natural hydrozincite from Hayden, Arizona, which was purchased from Ward's Natural Science Establishment, Inc., was used rather than commercial hydrozincite. All samples were used in the form in which they were purchased without crushing or acid pretreatment. The mineralogical purity of the materials was confirmed by comparing X-ray diffraction

* Present address: Schlumberger-GeoQuest, 1515 Poydras Avenue, Suite 900, New Orleans, Louisiana 70112, U.S.A. E-mail: mercy@new_orleans.geoquest.slb.com

TABLE 1. Steady-state and standard-state voltages from electro-chemical cell experiments used in calculating the Gibbs energies of formation and reaction

Cell	E(V)	E^0(V)	$m_2(m)$ (K_2CO_3)	$m_1(m)$ (KOH)	pH	$\gamma_{\pm}$ (KOH)	$\gamma_{\pm}$ (K_2CO_3)	ΔG_r^0 (kJ/mol)	ΔG_f^0 (kJ/mol)
1	0.6890	0.6640	0.050	0.050	12.7	0.737	0.525	−384.3	−1701.4
2	0.6771	0.6585	0.100	0.100	13.0	0.703	0.459	−381.2	−1698.3
A	0.6330	0.6390	0.208	0.109	13.0	0.679	0.407	−1823.7	−3150.7
B	0.6290	0.6390	0.104	0.054	12.7	0.703	0.467	−1818.9	−3149.1
C	0.6130	0.6250	0.052	0.027	12.4	0.740	0.536	−1775.9	−3134.8
D	0.6400	0.6460	0.208	0.109	13.0	0.679	0.407	−1838.8	−3155.8

(XRD) patterns to those of JCPDS reference samples no. 13-131 and no. 19-1458. Both the natural and synthetic hydrozincite were found to be pure, but XRD revealed the presence of minor amounts of $PbCO_3$(s) and $Pb(OH)_2$(s) in the hydrocerussite.

Electrochemical cells

We performed two sets of electrochemical cell experiments (Table 1). The first set, cells no. 1 and 2, were designed to determine values of ΔG_f^0 [$Pb(OH)_2 \cdot (PbCO_3)_2$(s)] and to establish the Pb(Hg)[2-phase]|$Pb(OH)_2 \cdot (PbCO_3)_2$(s)|$OH^-$(aq),$CO_3^{2-}$(aq) electrode (here referred to as the Pb-amalgam-hydrocerussite electrode) for use in later experiments. In a second set (cells A through D), we used the Pb-amalgam-hydrocerussite electrode as a reference electrode to determine values of ΔG_f^0 {$[Zn(OH)_2]_3 \cdot (ZnCO_3)_2$(s)}. Cell voltages were measured with a Tektronix DM 2510G digital multimeter calibrated with a Leeds and Northrup K-3 potentiometer and a bank of four standard cells, each of which was traceable to the National Institute of Standards and Technology (NIST).

Cell diagrams and cell reactions

The cell diagram for the cell used to determine ΔG_f^0 for hydrocerussite is:

$$\text{Pb(Hg)[2-phase]}|\text{Pb(OH)}_2 \cdot (\text{PbCO}_3)_2\text{(s)}|\text{KOH (aq, } m_1) \times \text{K}_2\text{CO}_3\text{(aq, } m_2)|\text{HgO(s)}|\text{Hg(1).} \quad (1)$$

The postulated half-reactions for these cells are:

$$3\text{Pb(Hg)[2-phase]} + 2\text{OH}^-(m_1) + 2\text{CO}_3^{2-}(m_2) \leftrightarrow \text{Pb(OH)}_2 \cdot (\text{PbCO}_3)_2\text{(s)} + 6\text{e}^- \quad (2)$$

and

$$6\text{e}^- + 3\text{HgO(s)} + 3\text{H}_2\text{O(1)} \leftrightarrow 3\text{Hg(1)} + 6\text{OH}^-(m_1). \quad (3)$$

The net cell reaction is:

$$3\text{Pb(Hg)[2-phase]} + 4\text{K}^+(2m_2 + m_1) + 2\text{CO}_3^{2-}(m_2) + 3\text{HgO}(s) + 3\text{H}_2\text{O(1)} \leftrightarrow \text{Pb(OH)}_2 \cdot (\text{PbCO}_3)_2\text{(s)} + 3\text{Hg(1)} + 4\text{K}^+(2m_2 + m_1) + 4\text{OH}^-(m_1) \quad (4)$$

where we have added $4K^+(2m_2 + m_1)$ to both sides of the equation so that the net reaction is written in terms of complete electrolytes. Application of the Nernst equation to the complete cell reaction yields:

$$E = E^0 - (RT/nF)\ln[a^4_{K^+(2m_2+m_1)} a^4_{OH^-(m_1)} / a^4_{K^+(2m_2+m_1)} \times a^2_{CO^{2-}_{3(m_2)}} a^3_{H_2O(l)}]. \quad (5)$$

Introducing mean activity coefficients (i.e.,

$$\gamma^2_{\pm KOH} = \gamma_{K^+} \cdot \gamma_{OH^-} \gamma^3_{\pm K_2CO_3} = \gamma^2_{K^+} \cdot \gamma_{CO_3^{2-}}),$$

and setting the number of electrons exchanged (n) equal to six to Equation 5 yields:

$$E = E^0 - (RT/6F)\ln[m_1^4/m_2^2] - (RT/6F) \times \ln[\gamma^8_{\pm KOH(aq,2m_2+m_1)} / \gamma^6_{\pm K_2CO_3(aq,2m_2+m_1)} a^3_{H_2O(l)}]. \quad (6)$$

Mean-ionic activity coefficients and H_2O activities are calculated using the Pitzer ion-ion interaction model (Plummer et al. 1988).

The free-energy change of the reaction, ΔG_r^0 is related to E^0 for the cell reaction by

$$\Delta G_r^0 = -6FE^0 \quad (7)$$

for reaction 4. From the cell reaction we have:

$$\begin{aligned}\Delta G_r^0 = {} & \Delta G_f^0[\text{Pb(OH)}_2 \cdot (\text{PbCO}_3)_2\text{(s)}] \\ & + 4\Delta G_f^0[\text{KOH(aq)}] + 3\Delta G_f^0[\text{Hg(1)}] \\ & - 3\Delta G_f^0[\text{Pb(Hg)}] - 2\Delta G_f^0[\text{K}_2\text{CO}_3\text{(aq)}] \\ & - 3\Delta G_f^0[\text{HgO(s)}] - 3\Delta G_f^0[\text{H}_2\text{O(1)}] \\ = {} & -6FE^0 \end{aligned} \quad (8)$$

from which ΔG_f^0[$Pb(OH)_2 \cdot (PbCO_3)_2$(s)] can be calculated.

The cell diagram for cells A through D is:

$$\text{Zn(Hg)[2-phase, saturated]}|[\text{Zn(OH)}_2]_3 \cdot (\text{ZnCO}_3)_2\text{(s)} \times |\text{K}_2\text{CO}_3\text{(aq, } m_2\text{), KOH(aq, } m_1)| \text{Pb(OH)}_2 \times (\text{PbCO}_3)_2\text{(s)}|\text{Pb(Hg)[2-phase].} \quad (9)$$

The postulated half-reactions, which involve the conversion of Zn to hydrozincite and the conversion of hydrocerussite to Pb are:

$$5\text{Zn(Hg)[2-phase, saturated]} + 6\text{OH}^-(m_1) + 2\text{CO}_3^{2-}(m_2). \leftrightarrow [\text{Zn(OH)}_2]_3 \cdot (\text{ZnCO}_3)_2\text{(s)} + 10\text{e}^- \quad (10)$$

and:

TABLE 2. Gibbs energies of formation values used in calculating ΔG_f^0 {$[Zn(OH)_2]_3 \cdot (ZnCO_3)_2(s)$}, $\Delta G_f^0[Pb(OH)_2 \cdot (PbCO_3)_2(s)]$, and equilibrium constants for Equations 17–20

Species	ΔG_f^0 (kJ/mol)	Source
HgO(s)	−58.40	Wagman et al. (1982)
Pb(Hg)[2-phase]	−1.13	Wagman et al. (1982)
Zn(Hg)[5%, saturated]	0.0	Wagman et al. (1982)
K_2CO_3(aq)	−1094.32	Wagman et al. (1982)
KOH(aq)	−440.50	Wagman et al. (1982)
$Pb(OH)_2 \cdot [PbCO_3]_2$	−1699.80	This study
Zn^{2+}(aq)	−147.260	Robie et al. (1978)
OH^-(aq)	−157.328	Robie et al. (1978)
CO_3^{2-}(aq)	−527.90	Robie et al. (1978)
$PbCO_3$(s)	−625.337	Robie et al. (1978)
$PbCO_3$(s)	−628.0	Taylor and Lopata (1984)
CO_2(g)	−394.375	Robie et al. (1978)
H_2O(l)	−237.18	Robie et al. (1978)

$$Pb(OH)_2 \cdot (PbCO_3)_2(s) + 6e^- \leftrightarrow 3Pb(Hg) + 2OH^-(m_1) + 2CO_3^{2-}(m_2). \quad (11)$$

The postulated net cell reaction is:

$$8KOH(aq, 2m_2 + m_1) + 15Zn(Hg) + 5Pb(OH)_2 \times (PbCO_3)_2(s) \leftrightarrow 15Pb(Hg)[2\text{-phase}] + 3[Zn(OH)_2]_3 \times (ZnCO_3)_2(s) + 4K_2CO_3(aq, 2m_2 + m_1) \quad (12)$$

where we add $8K^+(2m_2 + m_1)$ to both sides of the equation in order to express it in terms of complete electrolytes. Application of the Nernst equation to Equation 12 using mean activity coefficients and solution molalities yields:

$$E = E^0 - (RT/30F)\ln[m_2/m_1^2] - (RT/30F) \times [\gamma^3_{\pm K_2CO_3(2m_2 + m_1)}/\gamma^4_{\pm KOH(2m_2 + m_1)}]. \quad (13)$$

For this reaction, Equation 7 becomes

$$\Delta G_r^0 = -30FE^0. \quad (14)$$

From Equations 12 and 14 we obtain:

$$\begin{aligned}\Delta G_r^0 = {} & 3\Delta G_f^0\{[Zn(OH)_2]_3 \cdot (ZnCO_3)_2(s)\} \\ & + 15\Delta G_f^0(Pb(Hg)[2\text{-phase}]) \\ & + 4\Delta G_f^0[K_2CO_3(aq)] \\ & - 15\Delta G_f^0(Zn(Hg)[2\text{-phase, saturated}]) \\ & - 8\Delta G_f^0[KOH(aq)] \\ & - 5\Delta G_f^0[Pb(OH)_2 \cdot (PbCO_3)_2(s)] \\ = {} & -30FE^\circ. \end{aligned} \quad (15)$$

The ΔG_f^0 value for hydrocerussite together with the available ΔG_f^0 values for the other reactants and products in Equation 15 are listed in Table 2; these data are used to calculate the ΔG_f^0 value for hydrozincite. The cell reaction was demonstrated through Nernstian response of the electrode and through the absence of significant hysteresis in voltage vs. current reversibility tests. These tests involved measuring the voltage response of the cell to an applied current. The absence of hysteresis, as exhibited by a linear relationship between voltage and current, is considered strong evidence for reversibility in the cell reaction.

Cell construction

The electrochemical cells were constructed by methods described in Ives and Janz (1961) and Rock et al. (1994) and have no liquid-liquid junctions. The inside surfaces of the cell compartments were coated with Dow-Corning silicon fluid no. 200. Teflon-covered platinum electrode leads were inserted into the cells through small openings in the cell basins and were glued to the cells with Varian Torr-Seal epoxy. The platinum electrode leads were soldered to copper wires outside the cells. The region from the cell body to just below the platinum lead inside the cell was covered by melting small pieces of paraffin around the base of the cell compartment. In this way epoxy was isolated from the cell components.

The two-phase Pb amalgam (5 wt% Pb) and the two-phase Zn amalgam (saturated) were prepared in the laboratory for use in the cells. The Zn and Pb metals were first cleaned by soaking overnight in dilute (~0.01 *m*) nitric acid. Clean Hg was measured into clean glass containers and the appropriate amounts of metals were then added. The amalgams were then covered with argon and 0.01 *M* nitric acid, and then sealed and allowed to react. Approximately 2 g of metal amalgam were added to the appropriate cell compartments, which was enough to cover the platinum wire in each cell. After the amalgams were added to their respective cell chambers, each cell was filled with electrolyte solution and the solid phases were added. Table 1 shows the electrolyte composition for each cell. The experiments were performed with varying ionic strength in order to test Nernstian behavior. The solutions were prepared using reagent-grade KOH(s) and K_2CO_3(s), and the electrolyte concentrations were verified by analyzing for dissolved K using a Thermal Jarrell-Ash inductively coupled plasma atomic-emission spectrometer and by determining the hydroxyl-ion concentrations using a glass electrode. All solutions were stored under Ar to exclude CO_2. The solid salts were then added carefully to prevent migration of solids from one cell compartment to the other. After the solids were added, the cells were purged again with argon and then capped and sealed with Parafilm. We found no evidence of amalgam oxidation and the amalgams were mirror bright in the cell compartments.

Experimental conditions

Cells no. 1 and 2 were kept at laboratory temperatures until day 80 when they were placed in a bath at 25 ± 0.2 °C. The results reported are those obtained after the cells were placed in the temperature bath. In contrast, the hydrozincite cells (A through D) were stored continuously in a water bath maintained at 25 ± 0.2 °C. For cells A

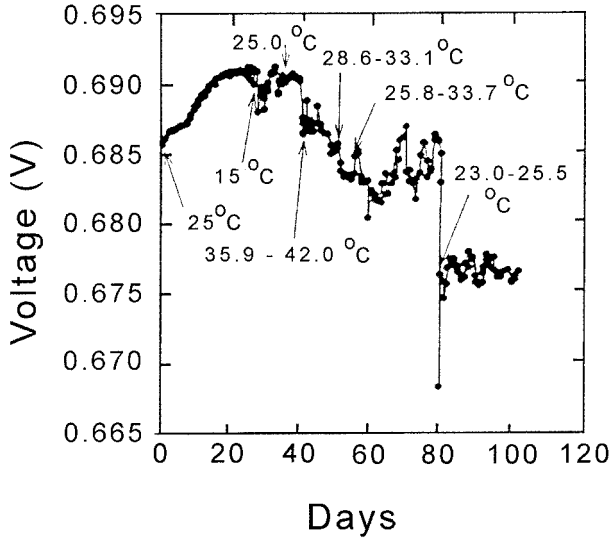

FIGURE 1. Voltage vs. time plot for cell 2.

through D, voltages were read every 12 h for the first 12 d and every 6 h for the remainder of the experiment (96 d total). Immediately following disassembly, the cell pH values were measured and the cell solution and solids were analyzed.

RESULTS

Hydrocerussite (cells 1 and 2)

Cell voltages rose sharply in both cells for the first 8 to 20 d. Cell no. 1 ($m_{KOH} = m_{K_2CO_3} = 0.050$ *m*) achieved a steady-state voltage around day 8 and maintained that voltage until approximately day 50, when the voltage began to slowly decrease. Periodic low-amplitude voltage fluctuations (~2–3 mV), whose cause was unknown, were observed from day 60 to day 80. For cell no. 2, a steady-state voltage was achieved after day 80 (Fig. 1) when the cell was placed in a 25.0 °C temperature bath.

The relatively large experimental drift in these cells undoubtedly relates to temperature fluctuations in the laboratory; a near-constant voltage value was reached after the cells were placed in a constant-temperature bath. The average steady-state voltages and solution compositions are reported in Table 1 for all cells.

Experiments to determine the cell reversibility involved determination of the reproducibility of the relation between cell voltage and current. We found small amounts of hysteresis (≈2 mV) in cell no. 1 (Fig. 2a), but very little hysteresis in cell no. 2 (Fig. 2b), indicating that the cell reaction is reversible to within the precision of our experiments.

The ΔG_r^0 values calculated for each cell (Table 1) using Equations 6 through 8 differ by only 0.15%, and the average values for ΔG_f^0 [$Pb(OH)_2 \cdot (PbCO_3)_2(s)$] = −1699.8 ±1.6 kJ/mol. Activity coefficients and other data used to calculate this value are compiled in Tables 1 and 2.

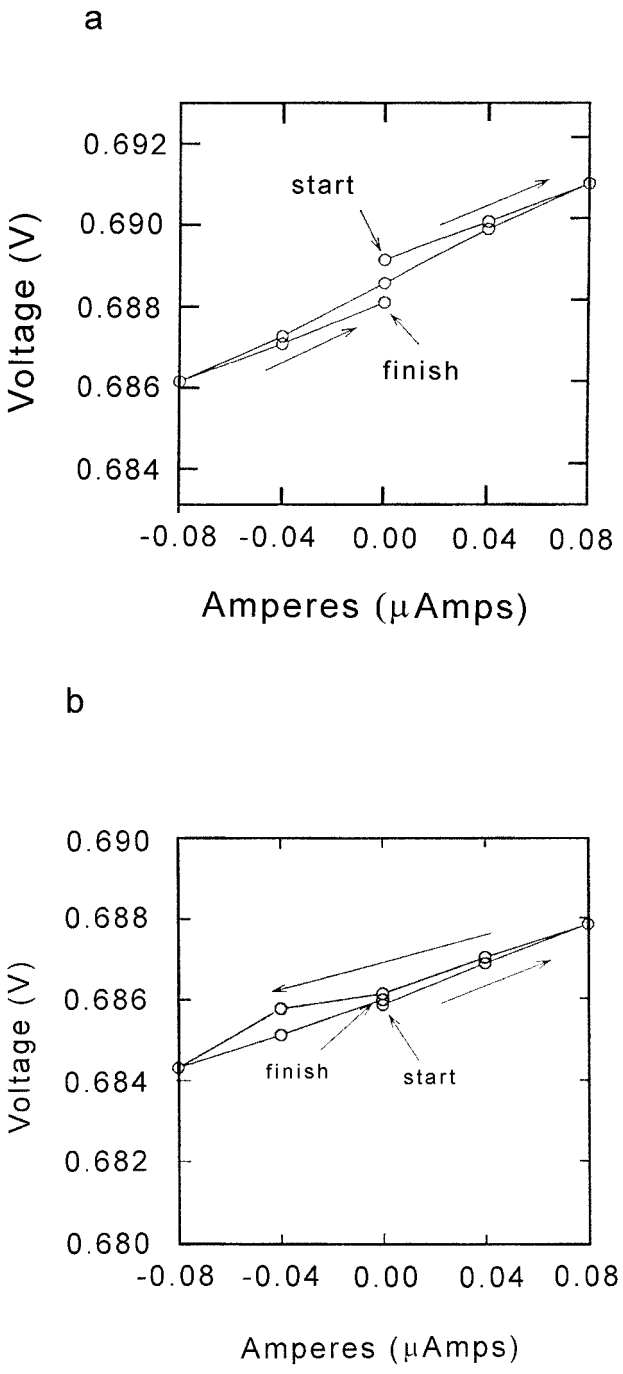

FIGURE 2. Voltage vs. current reversibility plot for (**a**) cell 1 and (**b**) cell 2.

Hydrozincite (cells A–D)

Cell voltages in the hydrozincite cells increased for approximately 10 d before reaching steady state. Once achieved, however, the steady-state voltage was nearly constant for a period of between 30 to 96 d (Fig. 3) after which each experiment was ended and the corresponding cell was disassembled. Steady-state voltages in cells A

through D allowed calculation of an average E and ΔG_r^0 using Equations 13 through 15. In determining the E values, only the voltages from the interval between 10–30 d were used because cells A and C became unstable after days 55 and 30, respectively. Cells B and D maintained steady-state voltages until disassembly, but only the time range 10–30 d was common to all cells.

Table 1 lists the ΔG_r^0 values calculated for each cell and their corresponding ΔG_f^0 values. These experiments with hydrozincite had much better temperature control than did the experiments with hydrocerussite, and thus the largest source of uncertainty in the estimates of ΔG_r^0 arises from estimates of the activities of KOH(aq) and K_2CO_3(aq). The estimated molalities of KOH(aq) and K_2CO_3(aq) vary by a factor of ≈2–5% over the long experimental times. These differences arise from slow drift in solution pH caused by dissolution of the solid and, perhaps, slow absorption of CO_2(g) into the solution through the cell cap. The drift was as large as 1.5 pH units only for cell C, which had the smallest buffering capacity. To bound the uncertainty in ΔG_r^0 values, we included this drift in electrolyte composition in our calculations. The initial electrolyte composition was well-constrained from the amount of KOH(s) and K_2CO_3(s) used to prepare the cell solutions. The composition at the end of the experiments was determined by analyzing the filtered electrolyte solution for pH and for dissolved K. The molalities of KOH(aq) and K_2CO_3(aq) could be calculated from this information. We assumed that the drift in molality with time was linear.

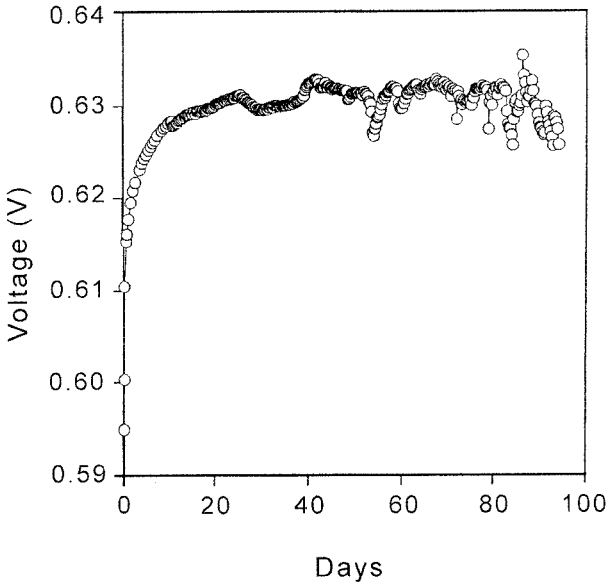

FIGURE 3. Voltage vs. time plot for cell B, which was typical of cells A–D.

DISCUSSION

Gibbs energies of hydrocerussite

Most values of ΔG_f^0[$Pb(OH)_2 \cdot (PbCO_3)_2$(s)] found in compilations of thermodynamic data (e.g., Latimer 1952; Naumov et al. 1974; Woods and Garrels 1987; Wagman et al. 1982) are traceable to the original solubility experiments of Randall and Spencer (1928) or to reinterpretation of this work by Garrels (1957). Garrels (1957) increased the value for ΔG_f^0[$Pb(OH)_2 \cdot (PbCO_3)_2$(s)] cited in Latimer (1952) by noting the relative abundance of cerussite and hydrocerussite in soils. The key geochemical reaction is:

$$3PbCO_3(s) + H_2O(l) \leftrightarrow Pb(OH)_2 \cdot (PbCO_3)_2(s) + CO_2(g). \quad (16)$$

In Equation 16, note that the equilibrium constant reduces to the activity of CO_2(g) for pure minerals and dilute water, which in most cases at the Earth's surface reduces to the partial pressure of CO_2 (P_{CO_2}).

The source of Latimer's (1952) estimate for ΔG_f^0 [$Pb(OH)_2 \cdot (PbCO_3)_2$(s)] was not given, but was probably from Randall and Spencer (1928), which was cited elsewhere in the Latimer (1952) text. The original Randall and Spencer (1928) work was a set of solubility experiments that required estimates of ΔG_f^0 values for other reactants and products to yield a value for ΔG_f^0 [$Pb(OH)_2 \cdot (PbCO_3)_2$(s)]. Naumov et al. (1974) interpreted the Randall and Spencer (1928) work to yield ΔG_f^0 [$Pb(OH)_2 \cdot (PbCO_3)_2$(s)] = −1711.0 kJ/mol. The original Randall and Spencer (1928) result required cerussite to be unstable relative to hydrocerussite at $P_{CO_2} \leq 10^{-1.8}$ atm. Garrels concluded that hydrocerussite must be stable at a much lower P_{CO_2} value, perhaps 10^{-4} atm, to account for the scarcity of this mineral relative to cerussite at the Earth's surface. Garrels (1957) reduced the ΔG_r^0 for Equation 16 by ~12 kJ/mol and this correction yields a ΔG_f^0 [$Pb(OH)_2 \cdot (PbCO_3)_2$(s)] = −1699 kJmol.

Two recent high-quality experimental efforts refined the value of ΔG_f^0 [$Pb(OH)_2 \cdot (PbCO_3)_2$(s)]. Taylor and Lopata (1984) reported ΔG_f^0 [$Pb(OH)_2 \cdot (PbCO_3)_2$(s)] = −1705 ± 11 kJ/mol from solubility experiments. Bilinski and Schindler (1982) also reported solubility experiments, though they did not present a value for ΔG_f^0 [$Pb(OH)_2 \cdot (PbCO_3)_2$(s)], and showed convincingly that the equilibrium for Equation 16 can be shifted to produce either cerussite or hydrocerussite at Earth surface conditions depending upon the choice of the speciation model for dissolved Pb. This sensitivity of solubility experiments to speciation models is avoided in the electrochemical cells that we employ here. Our experimental value for ΔG_f^0 [$Pb(OH)_2 \cdot (PbCO_3)_2$] = −1699.8 ± 1.6 kJ/mol is in close agreement with the values reported by Garrels (1957) and by Taylor and Lopata (1984).

Gibbs energies of hydrozincite

The ΔG_r^0 values for Equation 15 derived from cells A, B, and D lie within narrow range (±0.2% relative). The ΔG_r^0 value for cell C, which had the most-dilute electrolyte solution and therefore had the smallest pH-buffering capacity, was significantly lower (by 0.42% relative to

the others). Conducting the experiments at different ionic strengths (i.e., different activities of H_2O) provides a verification of Nernstian response. Our electrochemically determined value for ΔG_f^0 $\{[Zn(OH)_2]_3 \cdot (ZnCO_3)_2(s)\} = -3163.3 \pm 4$ kJ/mol (based on cells A, B, and D).

Schindler et al. (1969) reported experimental solubility products for the reaction:

$$Zn(OH)_{1.28}(CO_3)_{0.36}(s) = Zn^{2+}(aq) + 1.28\ OH^-(aq) + 0.36\ CO_3^{2-}(aq) \quad (17)$$

and:

$$Zn(OH)_{1.2}(CO_3)_{0.4}(s) = Zn^{2+}(aq) + 1.2\ OH^-(aq) + 0.4\ CO_3^{2-}(aq) \quad (18)$$

as $K_{sp} = 10^{-14.4}$ and $K_{sp} = 10^{-14.85}$, respectively, at I = 0.3 *m* (see also Zachara et al. 1989). To extract a Gibbs energy from this data, the solubility constants must be corrected by an activity coefficient model to infinite dilution, which we have not attempted to do here.

Alwan and Williams (1979) interpreted the chemistry of natural mine waters that were assumed to be in equilibrium with hydrozincite. They reported a solubility product for Equation 18 of $K_{sp} = 10^{-14.9 \pm 0.1}$. Conclusions from this field study depend strongly on the speciation model chosen to a greater extent than the solubility studies of Schindler et al. (1969) that were conducted with relatively simple solutions. When this experiment is reevaluated using thermodynamic data (Table 2), a value of ΔG_f^0 $\{[Zn(OH)_2]_3 \cdot (ZnCO_3)_8\} = -3161.5$ kJ/mol is obtained, which is in good agreement with our experimental value of ΔG_f^0 $\{[Zn(OH)_2]_3 \cdot (ZnCO_3)_8\} = -3163.3 \pm 4$ kJ/mol.

Paragenesis of hydrocerussite and cerussite in soil

Any explanation for the paragenesis of hydrocerussite must explain its relative rarity compared to cerussite in soils and the ease with which hydrocerussite is precipitated from experimental solutions at pH > 7. To account for the appearance of these minerals, we return to the analysis of Garrels (1957) and evaluate an equilibrium constant for Equation 16 using the value of ΔG_f^0 $[PbCO_3(s)] = -625.337$ kJ/mol from Robie et al. (1978) and other data compiled in Table 2. Using these values, we calculate $\Delta G_r^0 = 19.0$ kJ/mol (for Eq. 16), which corresponds to $K_{eq} = 10^{-3.33} = P_{CO_2}$. However, using the more recent value of ΔG^0_f $[PbCO_3(s)] = -628.0$ kJ/mol from Taylor and Lopata (1984), a value of $\Delta G^0_r = 27.0$ kJ/mol is obtained for Equation 16, which corresponds to $P_{CO_2} = 10^{-4.7}$ atm.

These P_{CO_2} values for equilibrium between cerussite and hydrocerussite straddle the prediction of Garrels (1957) of $P_{CO_2} = 10^{-4}$ atm and lie very close to the partial pressure of CO_2 in the atmosphere ($P_{CO_2} = 10^{-3.5}$ atm). Clearly, using the best available thermodynamic data, we cannot resolve which of these two solids, cerussite or hydrocerussite, forms from exposure of Pb minerals to the atmosphere.

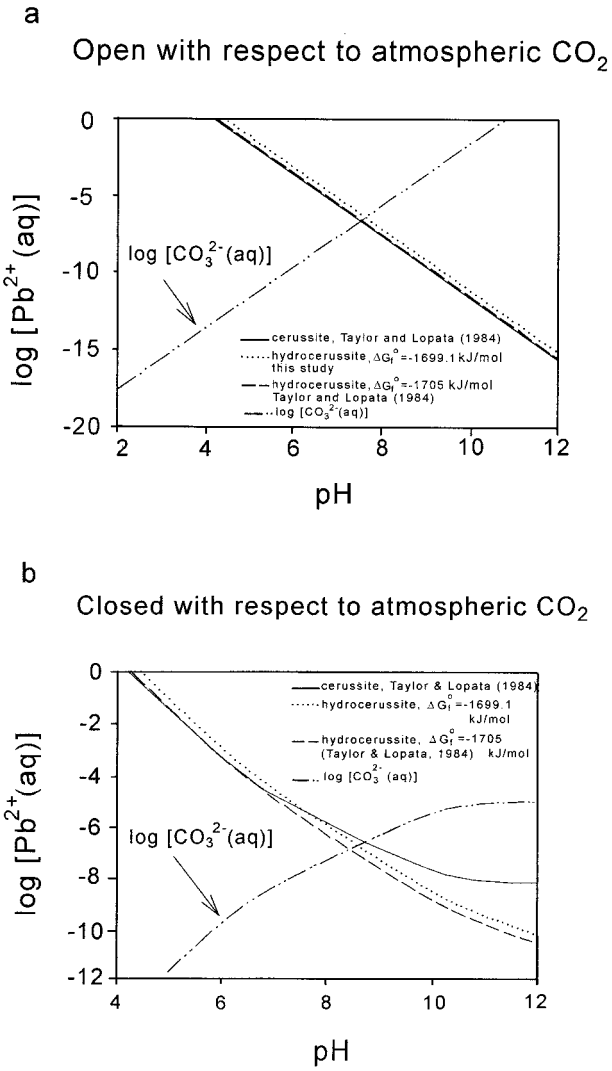

FIGURE 4. **(a)** The variation in the activity of $Pb^{2+}(aq)$ as a function of pH at $P_{CO_2} = 10^{-3.5}$ atm for a solution that is open to exchange of CO_2 with the atmosphere. The lines correspond to $Pb^{2+}(aq)$ activities in equilibrium with cerussite and hydrocerussite with two ΔG_f^0 $[Pb(OH)_2 \cdot (PbCO_3)_2(s)]$ values were used to illustrate the sensitivity of the result to the choice of thermodynamic data for hydrocerussite. The variation in the activity of $CO_3^{2-}(aq)$ is also shown. As one can see, hydrocerussite is always more soluble than cerussite, which is thermodynamically more stable. **(b)** The variation in the activity of $Pb^{2+}(aq)$ as a function of pH with a total dissolved carbonate concentration of 10^{-5} m for a solution that is closed to exchange of CO_2 with the atmosphere. The lines correspond to $Pb^{2+}(aq)$ activities in equilibrium with cerussite and hydrocerussite; the variation in the activity of $CO_3^{2-}(aq)$ is also shown. Hydrocerussite becomes considerably less soluble than cerussite at pH > 7 where the P_{CO_2} values are greatly reduced from $10^{-3.5}$ atm.

Hydrocerussite paragenesis, however, can be explained if the P_{CO_2} value of the weathering solution is not constant, but is well below the atmospheric value. The relative solubilities of cerussite and hydrocerussite as a func-

tion of pH are reversed if the aqueous solution is closed rather than open with respect to CO_2. Consider the speciation calculations shown in Figures 4a and 4b where the activities of Pb^{2+}(aq) and CO_3^{2-}(aq) are shown as a function of solution pH for solutions in equilibrium with cerussite and hydrocerussite. Inclusion of other species of dissolved Pb^{2+} would not change the essential result.

In Figure 4a, the P_{CO_2} value is fixed at the atmospheric level ($10^{-3.5}$ atm), and hydrocerussite is consistently more soluble; i.e., equilibration of hydrocerussite with this solution yields a higher activity of Pb^{2+}(aq) than does cerussite. The solubilities are, however, similar and can be reversed through a different choice of ΔG^0_f [$PbCO_3$(s)], as noted above. The important point is that one does not predict a change in the relative stabilities of cerussite and hydrocerussite for solids exposed to the atmosphere.

In contrast, a solution that is closed to exchange of CO_2(g) with the atmosphere has a higher variable P_{CO_2} value, which leads to a reversal of the relative stabilities of cerussite and hydrocerussite as pH increases (Fig. 4b). Hydrocerussite becomes more stable than cerussite at pH > 7 for a solution with a total dissolved carbonate concentration of 10^{-5} *m.* This solution corresponds to H_2O that was initially open to atmosphere and subsequently closed as pH increases. In summary, hydrocerussite forms from solutions where the P_{CO_2} value decreases with increasing pH. Closure could result from development of an armoring surface layer that is impervious to gaseous CO_2, or to depletion of the CO_2 through chemical reaction at a rate greater than it could be replenished through diffusion by the soil pores.

Acknowledgments

The authors thank Erin Walling, Minh Nguyen, and Dan Hebner for assistance with these experiments. We thank Patrick V. Brady, Liang Chai, and J. William Carey for their insightful reviews of this manuscript. This research was funded by grant no. DE-FG0392ER14307 from the Office of Basic Energy Science at the U.S. Department of Energy and by the Kearney Foundation grant no. 93-21.

References cited

Alwan, A.K. and Williams, P.A. (1979) Mineral formation from aqueous solution. Part I: The deposition of hydrozincite, $Zn_5(OH)_6)(CO_3)_2$, from natural waters. Transition Metal Chemistry, 4, 128–132.

Bilinski, H. and Schindler, P. (1982) Solubility and equilibrium constants of lead in carbonate solutions (25°C, i = 0.3 mol dm^{-3}). Geochimica et Cosmochimica Acta, 46, 921–928.

Brady, P.V., Brady, M.V., and Dorns, D.J. (1998). Natural Attenuation: CERCLA, RBCA's and the Future of Environmental Remediation, 245 p. Lewis Publishers, Boca Raton, Florida.

Garrels, R.M. (1957). Some free energy values from geologic relations. American Mineralogist, 42, 780–791.

Ives, D.J.G. and Janz, G.J. (1961). Reference Electrodes, 651 p. Academic Press, New York.

Jørgensen, S.S. and Willems, M. (1987). The fate of lead in soils: The transformation of lead pellets in shooting-range soils. AMBIO, 16, 11–15.

Latimer, W.M. (1952) Oxidation states of the elements and their potentials in aqueous solution, 392 p. Prentice-Hall, New Jersey.

Marani, D., Macchi, G., and Pagano, M. (1995) Lead precipitation in the presence of sulphate and carbonate: testing of thermodynamic predictions. Water Research, 29, 1085–1092.

Naumov, G.B., Ryzhenko, B.N., and Khodakovsky, I.L. (1974). Handbook of Thermodynamic Data. U.S. Geological Survey Report, USGS-WRD-74-001, 328 p.

Plummer, L.N., Parkhurst, D.C., Fleming, G.W., and Dunkle, S.A. (1988) A computer program incorporating Pitzer's equations for calculation of geochemical reactions in brines. U.S.G.S. Water Resources Investigations Report, 88-4153, 310 p.

Randall, M. and Spencer, H.M. (1928) Solubility of lead oxide and basic carbonate. Journal of the American Chemical Society, 50, 1572–1583.

Rickard, D.T. and Nriagu, J.O. (1978). Aqueous environmental chemistry of lead. In J.O. Nriagu, Ed., The Biogeochemistry of Lead in the Environment, p. 219–284. Elsevier-North-Holland Biomedical Press, New York.

Robie, R.A., Hemingway, B.S., and Fisher, J.R. (1978). Thermodynamic properties of minerals and related substances at 298.15 K and 1 bar (10^5 Pa) pressure and at higher temperatures. United States Geological Survey Bulletin, 1452, 456 p.

Rock, P.A., Casey, W.H., McBeath, M.M., and Walling, E.M. (1994). A new method for determining Gibbs energies of formation of metal-carbonate solid solutions: 1. The $Ca_xCd_{1-x}CO_3$(s) system at 298K and 1 bar. Geochimica et Cosmochimica Acta, 58, 4281–4291.

Schindler, P. Reinert, M., and Gamsjäger, H. (1969). Loslichkeitskonstanten und Freie Bildungsenthalpien von $ZnCO_3$(s) und $Zn_5(OH)_6(CO_3)_2$ bei 25°C. Helvetica Chimica Acta, 52, 2327–2332 (In German).

Smith, L.A., Means, J.L., Chen, A., Alleman, B., Chapman, C.C., Tixier, J.S. Jr., Brauning, S.E., Gavaskar, A.R., and Royer, M.D. (1995). Remedial options for metals-contaminated sites, 221 p. Lewis Publishers, Boca Raton, Florida.

Sperling, D. (1995). Future Drive: Electric Vehicles and Sustainable Transportation, 175 p. Island Press.

Taylor, P. and Lopata, V.J. (1984). Stability and solubility relationships between some solids in the system PbO-CO_2-H_2O. Canadian Journal of Chemistry, 62, 395–402.

Wagman, D.D., Evans, W.H., Parker, V.B., Schumm, R.H., Halow, I., Bailey, S.M., Churney, K.L., and Nuttall, R.L. (1982). The NBS tables of chemical thermodynamic properties: selected values for inorganic and C_1 and C_2 organic substances in SI units. Journal of Physical and Chemical Reference Data, 11, Supplement 2, 392 p.

Woods, T.L. and Garrels, R.M. (1987) Thermodynamic values at low temperature for natural inorganic materials: An uncritical summary, 242 p. Oxford University Press, U.K.

Zachara, J.M., Kittrick, J.A., Dake, L.S., and Harsh, J.B. (1989) Solubility and surface spectroscopy of zinc precipitates on calcite. Geochimica et Cosmochimica Acta, 53, 9–19.

Manuscript received July 31, 1997
Manuscript accepted February 4, 1998
Paper handled by J. William Carey